

# Influence of the inverter output circuit on the dielectric barrier discharges during the surface treatment of plastics

**Streszczenie.** Artykuł przedstawia model matematyczny oraz symulacyjny generator wyładowań barierowych (falownika z dopasowującym obwodem wyjściowym i komorą wyładowczą) stosowanego w procesie obróbki powierzchniowej polimerów. Zależności matematyczne oraz wyniki symulacji zostały użyte do zbadania wpływu parametrów obwodu wyjściowego falownika na jego charakterystyki sterowania. (Wpływ obwodu wyjściowego falownika na wyładowania barierowe w procesie powierzchniowej obróbki tworzyw).

**Abstract.** This article describes a mathematical and simulation model of the dielectric barrier discharge generator (inverter with its matching output circuit and discharging chamber) used in the treating process of polymer surface. Simulation model and mathematical relationships were used to investigate the influence of the inverter output circuit parameters on its control characteristics.

**Słowa kluczowe:** falownik rezonansowy, wyładowania barierowe, aktywacja powierzchni tworzyw.

**Keywords:** resonant inverter, dielectric barrier discharge, corona treatment of plastics surface.

## Introduction

In order to improve the adhesion of polymers during gluing, laminating and printing, dielectric barrier discharges (DBD, so-called corona treatment) are used to modify the surface. To achieve the desired level of adhesion energy of the order of 0,65-1,3kJ/m<sup>2</sup> should be delivered to the plastic. Parameters of corona treatment equipments are generally in the range of: power - 0.5...10 kVA, frequency - 5...50 kHz, voltage across the electrodes - 4...20 kV.

The equivalent circuit of a device for corona treatment of polymer foils is shown in Figure 1a. The main elements are: the unregulated or regulated (optional) DC power supply, inverter, transformer and discharge electrodes assembly. Discharges occur between the cylindrical (rotating) and rod (fixed) electrode. The electrodes and two dielectric layers (silicon and air) form a capacitor assembly. The third layer of dielectric is the treated plastic. Capacities of silicone and plastic layers are included in the further analysis as one capacitor. Capacities of the electrodes and the inductances (leakage inductance of the transformer and additional choke  $L_{dl}$ ) constitute a resonant circuit. The selection of transformer winding ratio (turns ratio) and of choke inductance allows operation of the system over a given frequency range, with the assumed output power. Figure 1b presents an equivalent circuit of the electrodes assembly while Figure 1c shows a simplified discharge characteristics  $i=f(u)$  in the air.

## Mathematical basis

According to the simplified scheme (Fig. 1b) and the characteristic of the discharge chamber (Fig. 1c) we can distinguish two states in operation of corona treatment equipments (Fig. 2): state 1, wherein there aren't discharges and the state 2 in which occur partial discharges (DBD discharges). In state 1 the voltage increase rate of  $u_C(q)$  on the discharge chamber terminals depends on the substitute capacity  $C_Z$  consisting of series-connected capacitors  $C_1$  and  $C_2$  (1). In state 2 the voltage on the capacitor  $C_2$  does not change, and the voltage increase rate of  $u_C(q)$  depends on the capacity  $C_1$  (2). On the basis of  $u_C(q)$  trajectory we can experimentally determine the parameters of the discharge chamber (Fig. 2).

$$(1), (2) \quad \frac{du_C}{dt} = \frac{1}{C_Z} = \frac{C_1 + C_2}{C_1 C_2}, \quad \frac{du_C}{dt} = \frac{1}{C_1}$$

Then the values of the chamber referred to the primary side of transformer are:  $C'_1 = g^2 C_1$ ,  $C'_2 = g^2 C_2$ ,  $C'_Z = g^2 C_Z$ ,  $U_p' = U_p/g$ , where:  $U_p$  - ignition voltage and discharge extinguish,  $g$  - transformer turns ratio. The frequency  $f_{syn}$  at the inverter output voltage and current synchronization, (taking into account the transformer turns ratio and the assumption that  $L_{dl} \gg L_\sigma$ ), is in the range  $f_{rmax} > f_{syn} > f_{rmin}$  (relationship 3 and 4).

$$(3) \quad f_{rmax} = \frac{1}{2\pi\sqrt{L_{dl}C_Z}g^2}$$

$$(4) \quad f_{rmin} = \frac{1}{2\pi\sqrt{L_{dl}C_1}g^2}$$

For the voltage and the frequency at which the voltage across the capacitor  $C_2$  does not reach the threshold voltage  $U_p$ , no current flows through the non-linear part of the load. In such conditions, the chamber is a linear load - the capacitor with capacity of  $C_Z$ . This capacitor together with choke  $L_{dl}$  creates a resonant circuit. This circuit has a low-pass filter properties, and the

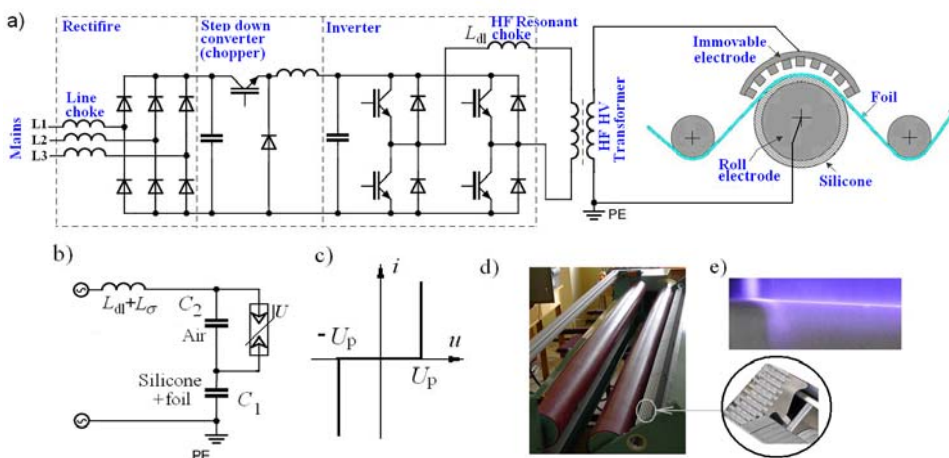


Fig.1. Equipment for treatment of polymeric film: structure (a), equivalent circuit of the load and its characteristic (b, c), view of the electrodes and discharges (d, e)

current flowing through it and the voltage on the equivalent capacitor  $C_z$  have the shape of a sine wave. In this case can be applied the classical analysis of sine waves.

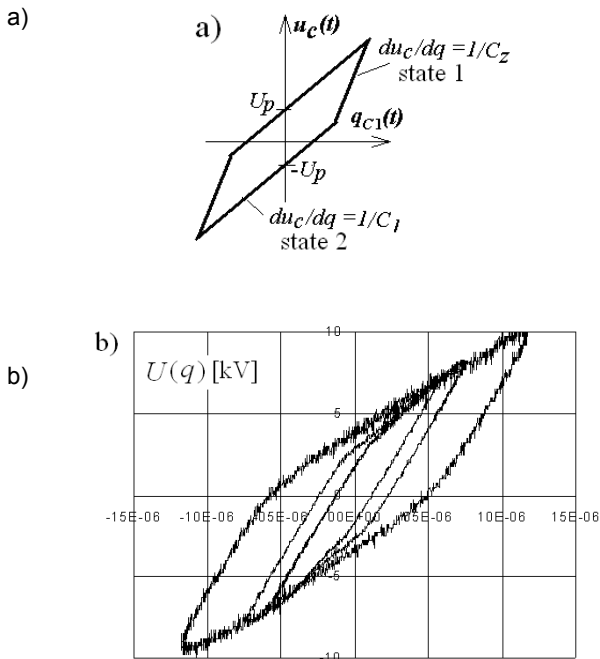


Fig. 2 Discharge voltage as a function of charge: a) illustration showing operating states, b) the trajectory obtained experimentally at three different frequencies of the inverter output voltage

The amplitude of the voltage across the capacitor  $C_2$  referred to the amplitude of the first harmonic of the inverter output voltage is described by relationships (5) - (7), wherein:  $U_{C2\_1m}$  - the amplitude of the voltage across the capacitor  $C_2$ ,  $U_{Inv\_1m}$  - the first harmonic amplitude of the inverter output voltage (in the full bridge circuit with a maximum duty cycle),  $\omega_s = 2\pi f_s$  - circular frequency of the inverter output voltage,  $f_s$  - transistors switching frequency.

$$(5) \quad \frac{U_{C2\_1m}/g}{U_{Inv\_1m}} = \left| \frac{1}{\omega_s^2 L_{dl} g^2 C_z - 1} \cdot \frac{C_z}{C_2} \right|$$

$$(6), (7) \quad U_{Inv\_1m} = \frac{4}{\pi} U_{dc}, \quad U_{C2m} = U_p \approx U_{C2\_1m}$$

The equation (7) determines when the amplitude of the voltage across the capacitor  $C_2$  reaches a value  $U_p$ . The limit values of the frequencies at which there are dielectric barrier discharges can be determined From equation (5) - (7):

$$(8) \quad f_{sgr1} = \frac{1}{2\pi} \sqrt{\frac{1}{L_{dl} g^2 C_2} \left( \frac{C_2}{C_z} - \frac{4U_{dc}}{\pi U_p / g} \right)},$$

$$(9) \quad f_{sgr2} = \frac{1}{2\pi} \sqrt{\frac{1}{L_{dl} g^2 C_2} \left( \frac{C_2}{C_z} + \frac{4U_{dc}}{\pi U_p / g} \right)}.$$

According to equations (8) and (9) discharges occur when  $f_{sgr1} < f_s < f_{sgr2}$ . The values of these frequencies depend not only on the capacity of the electrodes and the inductance of  $L_{dl}$ , but also on the ignition voltage, inverter output voltage and transformer winding ratio. Transformer winding ratio also affects the operating frequency range and power of the device. In reducing the inverter supply voltage these frequency limits approach to  $f_{rmax}$  (in accordance with 3, 8 and 9).

The relationships described above were confirmed experimentally (at one of the transformer winding ratio [1]) and by simulation tests. Characteristics of discharges power as functions of voltage and frequency are shown in Figure 3a, while Figure 3b shows characteristics of power, currents and voltages on the elements as functions of frequency at a constant inverter input voltage (300 Vdc).

Figure 3b, shows the frequency limits defined by the equations (3), (4), (8) and (9). Figures 3a and 3b are created by assuming a constant value of the transformer winding ratio and constant inductance  $L_{dl}$  ( $L_{dl} \gg L_{\sigma}$ ). In the simulation model was assumed parameters of the real system with power  $P_N = 3$  kW:  $U_{dc} \approx 300$  V, rotating electrodes: 2 pieces 1700x100 mm, 2 mm silicone insulation; immovable electrodes: 2 pieces 1600x36 mm toothed profile, capacitance  $C'_1 = 1.59$  nF,  $C'_2 = 0.794$  nF; air gap of approx. 2 - 4 mm (teeth);  $L_{dl} = 1.3$  mH; transformation windings ratio = 9.17. At the output of the inverter was connected an additional capacitor (having a relatively large capacity) to blocking a constant component in the current. This capacitor was taken into account in the computer simulation model.

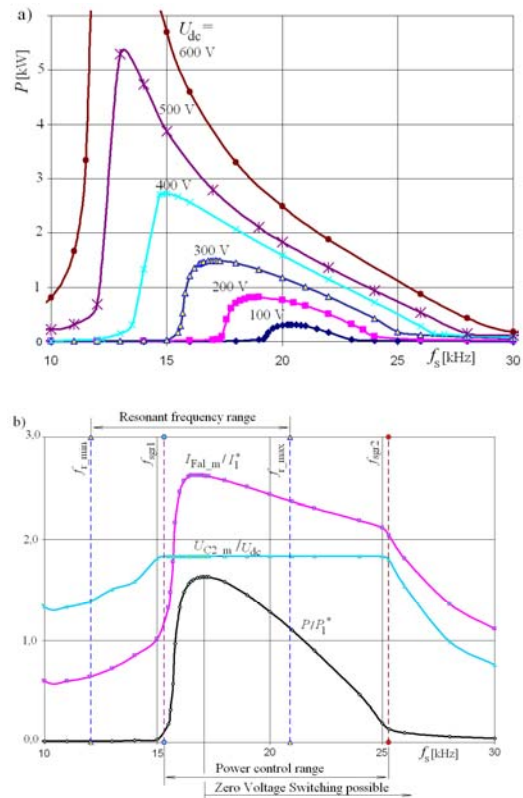


Fig. 3 Examples of discharge power characteristics (a, b), the maximum voltage across the capacitor  $C_2$  and the inverter output current (b) as a function of inverter output voltage frequency; the simulation results;  $I_1^* = U_{dc}/(L_{dl} C_1)^{1/2}$ ,  $P_1^* = U_{dc}^2/(L_{dl} C_1)^{1/2}$

Figure 4 shows the characteristics obtained by mathematical analysis (equation (8) and (9)) for the above written data. It is worth noting that the same values of frequency limits were obtained by simulation and analytically (points are marked on the characteristics of Figure 4). These frequencies coincide with the experimentally measured frequencies, wherein the differences do not exceed a few hundred hertz.

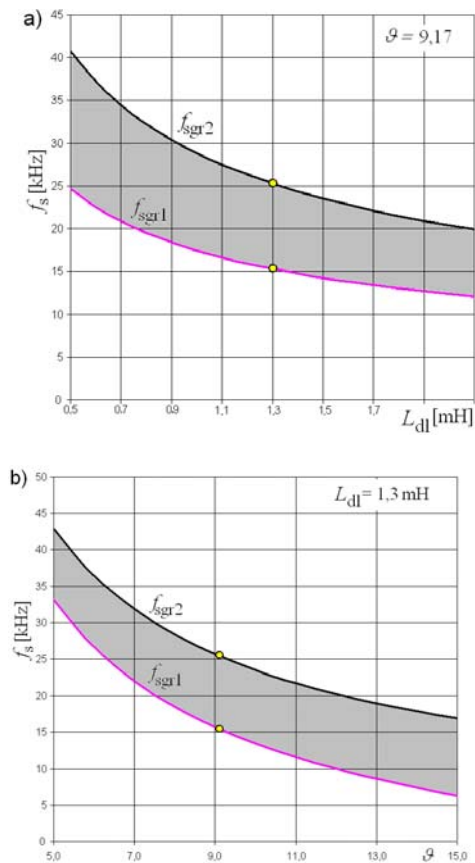


Fig. 4 Frequency limits defining the range of changes the transistor switching frequency at which the discharges appear; results of mathematical analysis; a) as a function of inductance  $L_{dl}$ , b) as a function of transformer windings ratio

**Influence of the inverter output circuit on the power control characteristics**

In previous works there has been no study of the impact of changes the transformer turns ratio and the series inductance  $L_{dl}$  on power control characteristics by DBD discharge system for surface treatment of plastics. The values of the turns ratio and the inductance were most frequently selected experimentally. The high demand for the equipment for processing different kinds of materials with different sizes (Fig. 6) resulted in the need to examine the impact of the transformer turns ratio and the inductance in the treatment process. Figure 4 shows the impact of inductance changes in resonant circuit and the transformer ratio on the frequency limits which define the range of frequency changes at the PFM modulation.



Fig. 6 Equipment for surface treatment of plastics by means of dielectric barrier (corona) discharge with generators (a) which were made on the basis of the author's documentation; processing of the film (b) and the adhesive label (c); elements of the lines was carried out in the Institute of Polymer Materials and Dyes Engineering (IMPIB) in Torun

Figure 5 presents the characteristics of the power control for the device with the same parameters as described above. It was assumed that the values of electrodes capacitance and voltage  $U_p$  are fixed. It should be noted that, with a change of the transformation ratio the values (referred to the inverter side) of the electrode capacities and voltage  $U_p$  also change.

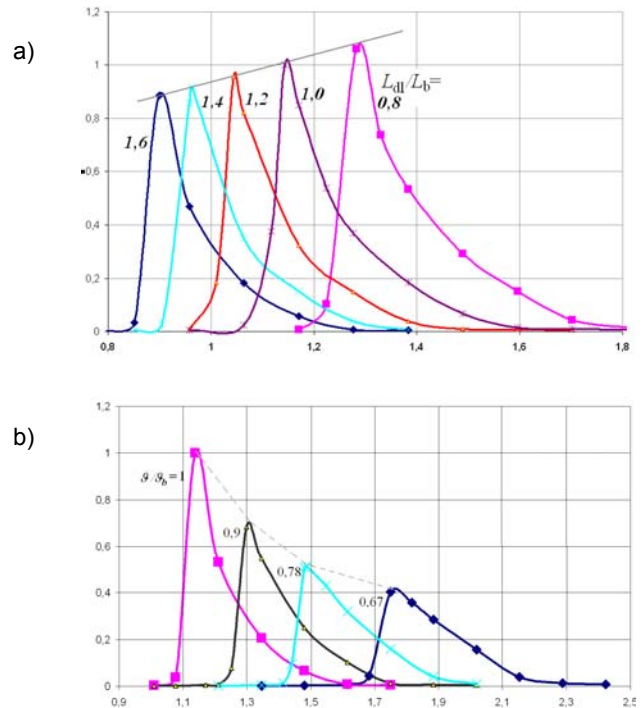


Fig. 5. Relative discharge power as a function of frequency for various inductance of the resonant circuit (a) and the transformer windings ratio (b);  $L_b=1\text{mH}$ ,  $g_b=9,17$ ,  $f_b=1/(2\pi(C_1L_b)^{1/2})$

Power control of the process [1, 2, 3] can be carried out using: pulse width modulation (PWM) - frequency modulation (PFM, see figure 3a, b, 5a, b), - voltage changes at the input of the inverter (PAM, Fig. 3a), - PDM modulation, - a combination of these methods. The impact of the parameter values of the output circuit of the inverter control characteristics (Specified by the author) is shown in Figure 5.

### Selected industrial applications

The devices for surface treatment of plastics by partial discharge DBD which were described in the article, are produced now on the basis of documentation and under the supervision of the author. Figure 6 presents the exemplary devices with generators developed by the author. The discharge chamber and technological lines (or parts of these lines) were performed at the Institute of Polymer Materials and Dyes Engineering (IMPiB, formerly Metalchem) in Torun.

### Conclusions

1. The article presents the mathematical description and simulation model of system for generation DBD discharges. Previous work of the author [1] confirms sufficient compliance of simulation results with those obtained experimentally, confirming the usefulness of the simulation model.
2. Simulation model and the mathematical relationships were used to examine the impact of the inverter output circuit on the frequency variation range of the generator (figure 4) and its control characteristics (Fig. 5).
3. Figure 5a shows that the maximum discharge power depends on the inductance and varies with frequency in a linear way. In contrast, points defining the maximum power as a function of the transformer windings ratio and frequency do not lie on a straight

line. Analytical determination of maximum power and the type of its variability will be the subject of future research of the author.

4. The article described generators for surface treatment of plastics by DBD discharges which are now produced on the basis of documentation and under the supervision of the author. One of the control methods of the generators has obtained patent protection [3].

### REFERENCES

- [1] Mućko J. Corona Treatment System with Resonant Inverter - Selected Properties. *13th International Power Electronics and Motion Control Conference (EPE-PEMC 2008)*, 1339-1343
- [2] Tsai M.T. Chu C.L. Power control strategies evaluation of a series resonant inverter for atmosphere plasma applications, *IEEE International Symposium on Industrial Electronics (ISIE 2009)*, 632-637
- [3] Mućko J.: Control method of resonant inverter for application of a foil treatment (Sposób sterowania falownikiem rezonansowym w zastosowaniu aktywności folii), - Patent no. P384865 (application / decision 07.04.2008 / 06.24.2013)

---

**Author:** dr hab. inż. Jan Mućko prof. UTP, University of Technology and Life Sciences in Bydgoszcz, Institute of Electrical Engineering, ul. Kaliskiego 7, 85-789 Bydgoszcz, Poland, E-mail: jan.mućko@utp.edu.pl